ACS OMEGA

http://pubs.acs.org/journal/acsodf

Article

Biophysical Investigation of the Interplay between the Conformational Species of Domain-Swapped GB1 Amyloid Mutant through Real−Time Monitoring of Amyloid Fibrillation

Renuka Ranjan, Nidhi Tiwari, Arvind M. Kayastha,* and Neeraj Sinha*

Cite This: *ACS Omega* 2021, 6, 34359−34366

Read Online

ACCESS | Metrics & More | Article Recommendations | Supporting Information

ABSTRACT: Mutant polypeptide GB1HS#124^{F26A}, which is known to aggregate into amyloid-like fibrils, has been utilized as a model in this study for gaining insights into the mechanism of domain-swapped aggregation through real-time monitoring. Size exclusion with UV monitoring at 280 nm and dynamic light scattering (DLS) profiles through different time points of fibrillation reveal that the dimer transitions into monomeric intermediates during the aggregation, which could further facilitate domain swapping to form amyloid fibrils. The 1D ^{1}H and 2D ^{1}H−^{13}C HSQC nuclear magnetic resonance (NMR) spectra profiling through different time points of fibrillation reveal that there may be some other species present along with the dimer during aggregation which contribute to different trends for the intensity of protons in the spectral peaks. Diffusion NMR reveals changes in the mobility of the dimeric species during the process of aggregation, indicating that the dimer gives rise to other lower molecular weight species midway during aggregation, which further add up to form the oligomers and amyloid fibrils successively. The present work is a preliminary study which explores the possibility of utilizing biophysical methods to gain atomistic level insights into the different stages of aggregation.

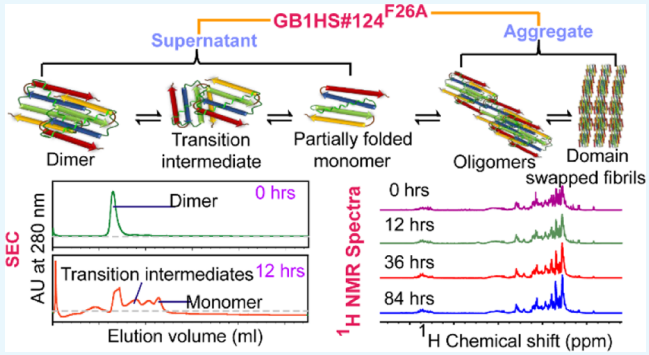

1. INTRODUCTION

Amyloid fibrils are causal agents of numerous forms of amyloidoses such as Alzheimer's and Parkinson's disease which are major health concerns worldwide.[1] Therefore, it is essential to probe for detailed information about the process of formation of such assemblies to develop a better understanding of this phenomenon, finding effective solutions to combat diseases, and to utilize such assemblies to human benefits. Different modes of fibrillation could be tracked down through its various stages to develop an understanding of the contribution of intermediates of fibrillation and oligomerization.[2,3] This could assist in detection of the toxic species and development of drugs which could bind to these species to inhibit the fibrillation and progression of amyloidosis into advanced stages.[4]

Domain swapping is one of the mechanisms of polypeptide folding into stable structures.[5] As the term suggests, similar domains are exchanged between subunits, and as a result, the polypeptide stabilizes into larger assemblies.[6−9] This phenomenon involves the unfolding of domains causing a destabilized structure which folds back together with the identical domains of another subunit resulting in a lower energy highly stable oligomer.[2,7,10] These oligomers further domain swap through these intermediate states to polymerize. This phenomenon is exhibited by a number of polypeptides which could form amyloid fibrils.[11−15] A number of mutants of immunoglobulin-binding B1 domain of protein G, a streptococcal protein show propensity to aggregate into amyloid fibrils,[16−19] one of which is GB1HS#124^{F26A}. This mutant, along with other hydrophobic core mutants, had been designed by Gronenborn et al. through back mutation of phenylalanine at the 26th position in the tetramer mutant sequence of protein GB1 (mutations L5V, F30V, Y33F, and A34F) to alanine.[19] These mutant polypeptides served as a model to study the folding mechanism of polypeptides under different temperature and pH conditions, out of which GB1HS#124^{F26A} was found to oligomerize through a domain-swapping mechanism. It is known to exist as a dimer in equilibrium with a partially folded monomer.[20] Extensive studies on this mutant employing various biophysical methods have revealed that it forms amyloid-like fibrils through domain swapping where peripheral strands of dimers are recruited to oligomerize into amyloid

Received: August 6, 2021
Accepted: November 23, 2021
Published: December 7, 2021

ACS Publications

© 2021 The Authors. Published by American Chemical Society

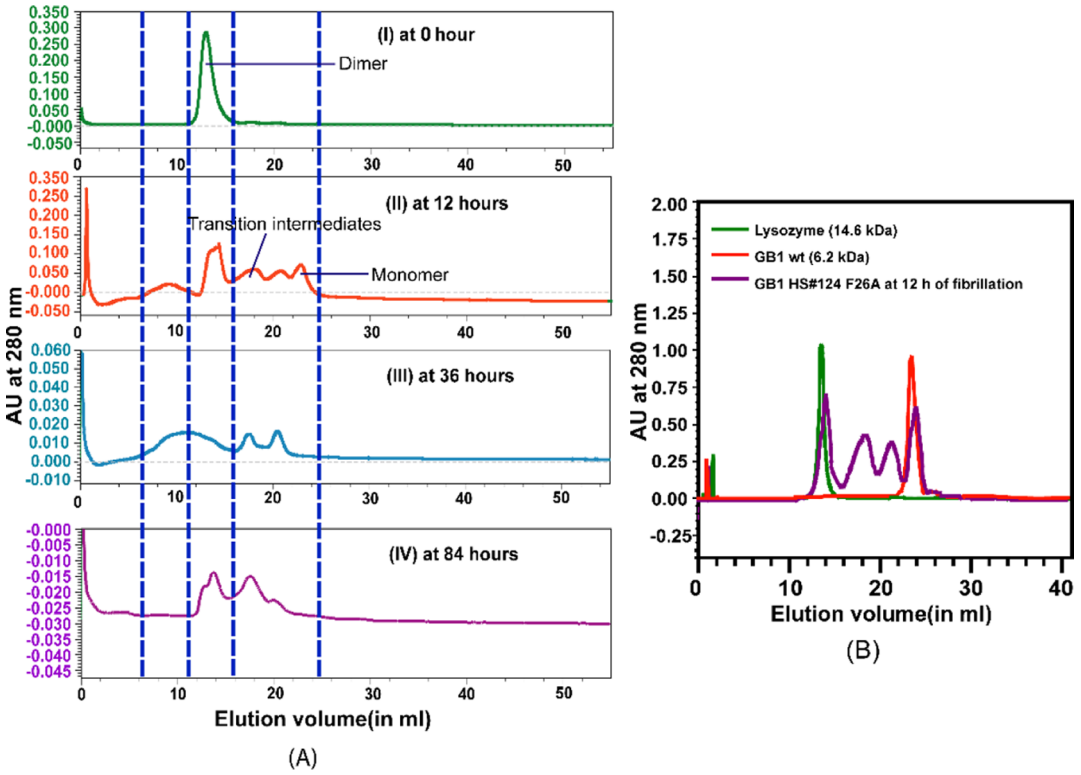

Figure 1. (A) Size-exclusion chromatogram for GB1HS#124^{F26A} during fibrillation at time points (I) 0 h or the start point of incubation (II) 12 h, (III) 36 h, and (IV) 84 h. (B) Elution profile of lysozyme (14.6 kDa) and wt GB1(6.2 kDa) run as standards to confirm the size of dimeric and monomeric species of GB1 HS#124^{F26A}

fibrils.[21,22] Biophysical analyses and molecular simulations of many other variants of GB1 have also been frequently utilized to understand folding−unfolding mechanisms of polypeptides forming such supramolecular assemblies.[23,24] A number of nuclear magnetic resonance (NMR)-based methods for polypeptides in solutions and solids have been utilized in an effort to understand the domain-swapping mechanism.[19−22,25,26] These studies suggest a possibility of the generation of a destabilized intermediate with increased conformation inhomogeneity for a part of the polypeptide during the process of domain swapping.[10,20]

High-throughput experimental techniques such as circular dichroism, dynamic light scattering (DLS), and size-exclusion profiling have been extensively utilized to develop a better understanding of the mechanism of amyloid fibrillation.[23,27] Size-exclusion chromatography (SEC) separates polypeptides on the basis of their molecular weight, and thus could identify the number of subunits in the eluted fractions.[28] Transition intermediates can also be detected by profiling size-exclusion through UV−vis absorbance. DLS can efficiently track down the hydrodynamic radii of the constituent molecules in the protein solution and has been used widely to study amyloid fibrillation.

In recent times, several strategies have been fortified to study various aspects of amyloid fibrillation using NMR.[3,29,30] Solution NMR is extensively used for studying the structure, function, and dynamics of polypeptides and thus proves to be an excellent technique in studying aggregation of amyloidogenic polypeptides.[31−34] In recent times, advanced NMR technologies such as high magnetic field experimentation and dissolution dynamic nuclear polarization have paved way to attain a higher-resolution insight into the fibrillation mechanism using solution NMR spectroscopy.[35,36] A study by Krishnamoorthy et al. employed CPMG-based relaxation dispersion of side chains of amyloid-β (1−40) to track their dynamics during amyloid fibrillation.[37] Another study by Wang et al. mentions the use of ^{1}H magic angle spinning (MAS) NMR to monitor aggregation of proteins in real time in a solution state.[38] A plethora of NMR experiments such as CPMG relaxation transfer, off-resonance R1ρ relaxation, lifetime line broadening, dark-state exchange saturation transfer, and paramagnetic relaxation enhancement have been employed in recent studies to track down intermediates of amyloid fibrillation in real time.[3,39]

The present study harnesses potential of NMR spectroscopy and SEC along with DLS to probe into the aggregation mechanism of GB1HS#124^{F26A}.[40−42] A thorough profiling of diffusion coefficients of side-chain protons at various time points may imply a correlation between changes in diffusion coefficient and aggregation.[40−42] Furthermore, the effect of domain-swapped aggregation of GB1HS#124^{F26A} polypeptide on spin−lattice relaxation could be suggestive of the rotational or vibrational motions occurring in side-chain-attached protons which could further form basis for the study of motional behavior of side-chain-attached protons due to other factors such as spin diffusion and chemical exchange.[41−43] The present research employs quick and economical methods to study the aggregation mechanism of polypeptides which undergo domain swapping to form amyloid fibrils.

2. RESULTS AND DISCUSSION

2.1. Detection of Intermediates of GB1HS#124^{F26A} during Fibrillation by Observing SEC Elution and DLS Profiles. It has been proven in previous studies[19−21] that the

https://doi.org/10.1021/acsomega.1c04223
ACS Omega 2021, 6, 34359−34366

GB1HS#124^{F26A} polypeptide exists in a native state as a domain-swapped dimer in equilibrium with a partially folded monomeric species, where dimers are indicated to be the constituting units of the amyloid fibrils. The mechanism of aggregation and the conformational species (monomers, dimers, or oligomers) of GB1HS#124^{F26A} aggregating to form the amyloid-like fibrils has been elusive and needs to be probed further.[22] Size-exclusion chromatogram at various time points during fibrillation (Figure 1) clearly shows that the dimers and monomers along with some transition intermediates are present in the protein solution, which might afterward add up to form oligomers and amyloid-like fibrils successively. At the start of fibrillation (0 h), the polypeptide exists in a dimeric conformation. After incubation of the protein at 58 °C with agitation for ∼12 h, oligomers appear in the solution, as shown by the elution profile along with the dimer (elution volume 14 mL) and other lower molecular weight transition intermediates (elution volume 18−20 mL) and monomer (elution volume 23 mL). In previous studies,[19−21] the monomer has been reported to exist in a partially folded form. Denotation of peaks for dimer and monomer has been confirmed by running standards of lysozyme (14.5 kDa) and wt GB1 (6.2 kDa) on a size-exclusion column under same buffer conditions (Figure 1B). After 36 h of incubation, the peak for the monomeric species is completely lost along and chromatogram peaks only show oligomeric, dimeric, and the transition intermediates. After 84 h of fibrillation, the only soluble species remaining are dimer and the intermediate species which could be present in equilibrium with the fibrillar state. A similar observation could also be deduced by the Tris-tricine SDS-PAGE of the supernatant of GB1HS#124^{F26A} (see Supporting Information S1).

Furthermore, these observations correspond to DLS analysis which shows the soluble species present in the polypeptide solution at successive stages of fibrillation. Figure 2 shows the hydrodynamic diameter profile of lower molecular weight soluble species of GB1HS#124^{F26A} using DLS at 0, 12, 36, and 84 h of fibrillation (referred to as DLS profile). At 0 h, the size of the species shown by a single peak is 46 ± 12 nm. This peak indicates dimer species present in the solution. At 12 h of fibrillation, three peaks are visible in the light scattering profile which fall in the size range 26.49 ± 7.3, 36 ± 22.3, 59 ± 32.2, and 792 ± 105.2 nm. These peaks correspond to monomers, intermediate species, and dimeric species, respectively, when compared with size-exclusion chromatogram (Figure 1). At 36 h time point, peaks with hydrodynamic diameter of 14 ± 4.3, 41 ± 7.7, 71 ± 11.3, and 1200 ± 396.4 nm values are shown in the DLS profile which vary in intensity. These peaks correspond to same composition as that of the species observed in the size-exclusion chromatogram, except for the presence of monomer. At 84 h time point, peaks representing the diameter of remaining soluble species as 24.4 ± 13.2, 37.4 ± 15.2, and 57 ± 20.3 2 nm were obtained, which correspond to the monomer intermediate and dimeric species.

An explanation to these trends in the elution profile over time is that the dimer converts into a partially folded monomeric state or open monomers through some transition intermediates, which could then either transition back to the dimeric state or simply aggregate to form oligomers, protofibrils, and amyloid fibrils successively. Thus, the elution profile of the GB1HS#124^{F26A} confirms the transition of a closed dimer into an open state (transition intermediates and partially folded monomers) which provides the indication of

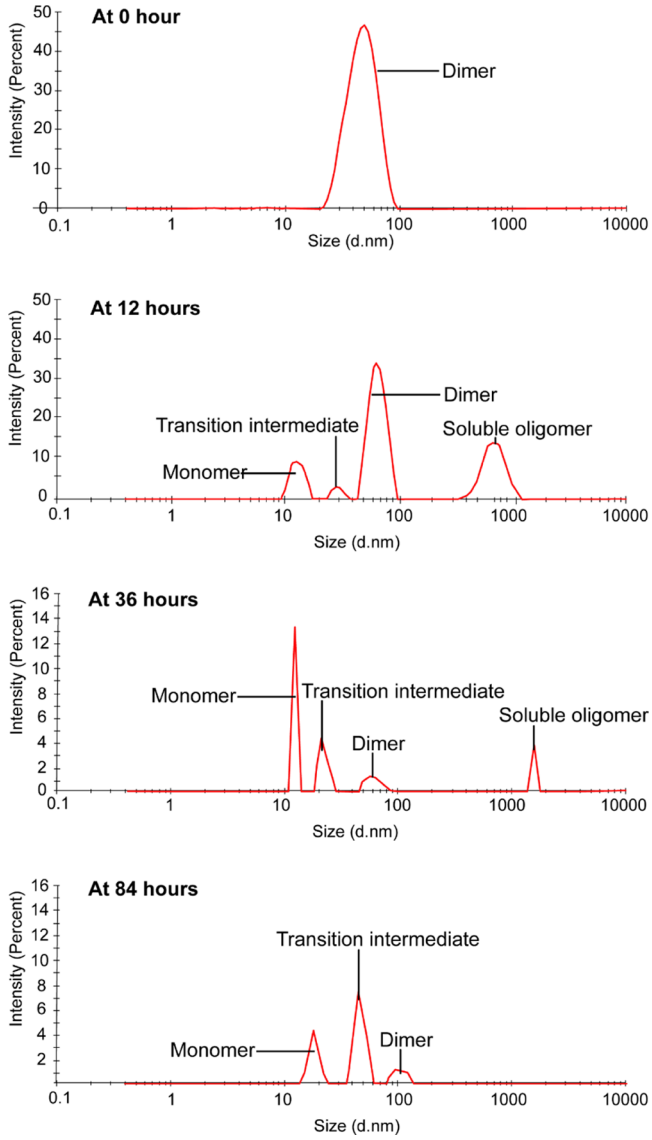

Figure 2. DLS profile of GB1 HS#124^{F26A} depicting lower molecular weight soluble species present at time points 0, 12, 36, and 84 h of fibrillation.

domain-swapping mechanism occurring during the fibrillation of GB1HS#124^{F26A} into amyloid fibrils. The elution profile could have been different if the fibrillation could have occurred through modes other than domain swapping. There would have been a constant decrease in concentration of initial species without the appearance of other lower molecular weight intermediates, had the fibrillation been occurring through mechanisms other than domain swapping. The elution profiles at these time points, therefore, provide a glimpse into the key conformational species of GB1HS#124^{F26A} polypeptides involved in the aggregation mechanism through domain swapping.

2.2. Role of Side-Chain-Attached Protons in Fibrillation through the Domain-Swapping Mechanism. Maintaining fibrillation conditions for the protein in a solution (temperature and pH) during NMR experiments for aggregation could provide a glimpse into the real-time changes in the microenvironment of the polypeptide and structural changes at atomistic levels while undergoing aggregation. Therefore, all NMR experiments were recorded at 58 °C and

https://doi.org/10.1021/acsomega.1c04223
ACS Omega 2021, 6, 34359−34366

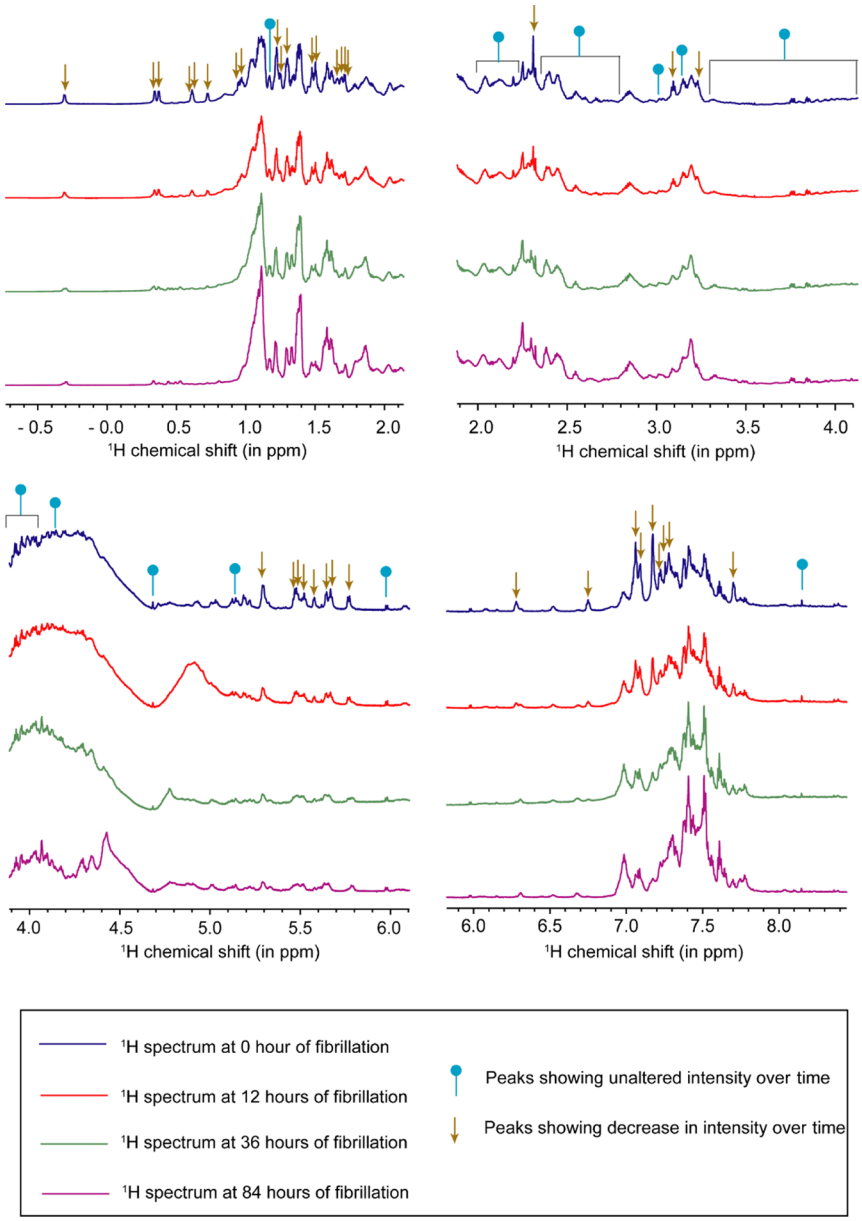

Figure 3. 1D ^{1}H NMR spectra of GB1HS#124^{F26A} at 0, 12, 36, and 84 h of fibrillation at 58 °C and pH = 5.5.

sample pH = 5.5 in sodium phosphate buffer. A concentration of 0.6 mM was chosen as concentrations higher than this resulted in a faster aggregation, and thus could not provide a suitable time window to carry out all the NMR experiments with ease.

Previous studies[21] suggest an active role of side chains of a few amino acids in the fibrillation of GB1HS#124^{F26A}. To identify and assign side-chain ^{1}H chemical shifts at 58 °C, the existing data for the ^{1}H and ^{13}C nuclei chemical shift assignment of GB1HS#124^{F26A} polypeptide from BMRB, and the recorded 1D ^{1}H NMR data at 25 °C were matched and compared to that of the 1D ^{1}H and 2D ^{1}H−^{13}C HSQC NMR spectra of GB1HS#124^{F26A} at 58 °C in pure D_2O, as other type of protons (amide and hydroxide) get exchanged with deuterium and are not visible in ^{1}H NMR spectra. Assignments of 247 proton peaks out of 362 ^{1}H chemical shifts mentioned in the BMRB database with accession number 5875 were obtained in the spectra at 58 °C (see Supporting Information Table S2). Cross-peaks in ^{1}H−^{13}C HSQC provide chemical shifts of ^{1}H and ^{13}C nuclei and these further confirm the assignment of ^{1}H chemical shifts obtained for the GB1HS#124^{F26A} polypeptide at 58 °C. These experiments were continued throughout the course of fibrillation recorded at time points 0, 12, 36, and 84 h, and a profile of 1D ^{1}H NMR spectra (Figure 3) show changes in side-chain-attached protons during fibrillation.

Changes in the intensity of peaks in 1D ^{1}H spectra through the course of fibrillation were found to be least prominent in the region of 4−6 ppm which mainly contains peaks for protons attached to α-carbons of the amino acid side chain. These changes were more noticeable in the region of 0−2 ppm (containing peaks mostly for protons attached to γ- and δ-carbons), 2−4 ppm (containing peaks mostly for protons attached to β-carbons), and 6−8 ppm (containing peaks mostly for protons attached to aromatic ring carbons), as evident from the assignment of the peaks in ^{1}H−^{13}C HSQC spectra. This suggests that the intensity changes of the protons are affected by their position in the side chain, and thus could

https://doi.org/10.1021/acsomega.1c04223
ACS Omega 2021, 6, 34359−34366

be an objective for studying the motional dynamics during the process of domain-swapped fibrillation.

During fibrillation by a nucleation dependent mechanism, the intensity of the proton peaks in the NMR spectra continues to decrease over time. In the present case, the changes in intensity of the protons are not uniform throughout the spectra during fibrillation observed at the four time points. There is an observable decrease in intensity and increase in line width for peaks at −0.30, 0.34, 0.37, 0.608, 0.618, 0.72, 0.94, 0.96, 1.19−1.26, 1.29, 1.47, 1.49, 1.66, 1.68, 1.70, 1.71, 2.3, 3.08, 3.20−3.23, 5.29, 5.45−5.68, 5.7, 6.28, 6.74, 7.06, 7.09, 7.15−7.28, and 7.7 ppm. Increase in intensity accompanied with decrease in line width is another observable trait for certain peaks at 0.44, 0.51, 0.81, 1.0−1.14, 1.32, 1.33, 1.35−1.40, 1.54−1.63, 1.74−1.89, 2.83, 3.17, 6.98, 7.29−7.53, and 7.61 ppm. Peaks at 1.16, 2.0−2.23, 2.35−2.77, 2.9, 3.13, 3.34−4.08, 4.18, 4.6, 5.12, 5.96, and 8.17 remain unaltered in intensity or line width.

Furthermore, analysis of 2D $^{1}H-^{13}C$ HSQC NMR spectra (see Supporting Information S3) recorded at the same time points during fibrillation confirm trends observed in the 1D ^{1}H spectral profiles. Distinct cross-peaks were used to track changes in the intensity of peaks assigned to the protons attached to the side-chain carbon. On observing the cross-peaks assigned to the dimer, it is clear that these peaks show decrease in intensity more often. The assigned dimeric peaks show increase in intensity only in the regions where there is an overlap of ^{1}H chemical shifts (as indicated in Table S2). Certain other unassigned peaks which do not experience any overlaps by signals from the dimers show a similar increase in intensity. This provides a clue that the peaks experiencing an increase in intensity through the course of fibrillation could be of the oligomeric origin.

Yet, some other unassigned peaks appear at 12 h time point onward and decrease in intensity at 84 h ($\delta_{ppm}(^{1}H,^{13}C)$ = 0.37, 24.04; 1.07, 19.92; 1.11, 21.28; 1.74, 30.01; 1.77, 30.05; 3.07, 36.61; 3.35, 36.3; 4.4, 53.54; 4.45, 59.59; 4.51, 50.42; 4.75, 51.88; 5.17, 59.56; 5.29, 101.11; 6.90, 115.59; 7.30, 127.22). These peaks could be signals arising from the intermediate species or the partially folded monomer, which could be delineated further to track their origin, using advanced NMR methods that employ robust labeling strategies.

The observations made in 1D ^{1}H and 2D $^{1}H-^{13}C$ HSQC are, thus, suggestive of the presence of other conformational species along with the dimer, apart from the presence of oligomers in a solution during the course of fibrillation. These conformational species, however, could not be delineated using these methods and would require high resolution NMR methods to further differentiate between the intermediates formed during the fibrillation.

A few distinctive peaks for dimers which do not merge with other peaks and continue the drop in intensity could be used for quantification of the polypeptide in order to track aggregation (e.g., peaks for HG 11, 12, 13, 21, 22, 23 of V54, HD 11, 12, 13, 21, 22, 23 of L12, HG 21, 22, 23 of V5, HG 21, 22, 23 of V30, etc.). Some other peaks which remain unaltered in the chemical shift, line width, and intensity peaks can be used for the purpose of quantification of initial concentrations of the polypeptide before it underwent aggregation. After entering the stationary phase of fibrillation, there is no further change observed in 1D ^{1}H spectra after 84 h of aggregation.

2.3. Diffusion Coefficient Trends Confirm Destabilization of the Native Domain-Swapped Dimer during the Process of Fibrillation.

Diffusion measurements for each of the side-chain proton peaks were carried out at time points 0, 12, 36, and 84 h, respectively. Diffusion coefficients were calculated for all the assigned and distinct dimeric chemical shift of protons (see Table S4). Mean values of diffusion coefficient were calculated at each of the chosen time points which altogether represents the motion of the initially abundant dimer of the polypeptide over the course of fibrillation. Figure 4 shows a bar diagram of mean diffusion coefficient values which reflects changes in the trend of diffusion coefficient during the process of fibrillation.

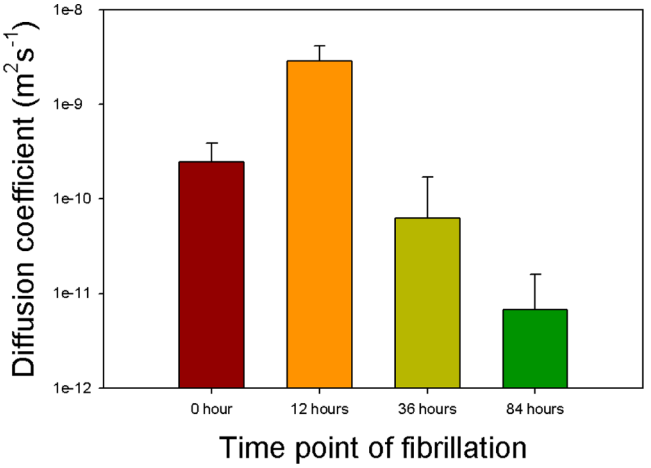

Figure 4. Changes in the mean diffusion coefficient during fibrillation measured at time point 0, 12, 36, and 84 h, respectively.

For the side-chain-attached protons, the diffusion coefficient increases by an order of magnitude of 10^{1} after 12 h of fibrillation. Thereafter, the diffusion coefficient decreases drastically in order of magnitude 10^{-2} at 36 h of fibrillation which further continues to decrease at 84 h of fibrillation (a drop of 10^{-1} order of magnitude). Therefore, a trend of diffusion coefficient is observed where it rises during 12 h of fibrillation, and then decreases sharply and then continues to decrease after 36 h to the final time point of fibrillation. This trend is suggestive of destabilization of a stable dimer and appearance of transition species which could further aggregate into amyloid fibrils. Increase in the diffusion coefficient corresponds to increase in the translational motion which could occur as a result of unfolding of the dimer into more mobile and unstable intermediates (open monomers and dimer).[41] Molecular dynamic simulation studies have hinted toward the propensity of dimer destabilization of GB1HS#124^{F26A}.[24] Thus, the theory that the dimers unfold into destabilized monomers and further aggregate into fibrils finds another proof by observation of these trends.[21]

Diffusion NMR can be further utilized to calculate hydrodynamic radii of the protein which could serve as a determinant of the degree of folding of the polypeptide. Diffusion NMR is also a tool to track the self-association of polypeptides.[46] The structure or shape of the polypeptide in question shall be predetermined prior to the application of diffusion NMR methods, which limits this method to be applied to novel proteins undergoing aggregation.

2.4. High T_1 Relaxation Time Values Related to the Separation of the Intermediates during Size Exclusion.

The separation of the intermediates as shown in the size-

https://doi.org/10.1021/acsomega.1c04223
ACS Omega 2021, 6, 34359−34366

exclusion profiles at each time point could be explained by probable slow-exchange rates of the intermediates which have larger values than the rate of elution of these conformational species.[19,20] This is hinted by the T_1 relaxation times calculated for the side-chain protons (see Supporting Information S5) which shows highly ambiguous and out of range values. The trends for T_1 values calculated for the dimeric chemical shifts assigned to the side-chain-attached protons show aberrations, as the calculated T_1 values are higher than the expected values on the basis of recycle delay (recycle delay should be $5T_1$) provided for each T_1 relaxation experiment. It may be concluded that these motions of side-chain-attached protons is not only rotational or vibrational in nature but are also occurring at a scale higher than picoseconds to nanoseconds which could be governed by other factors such as conformational change or slow chemical exchange. As observed by Byeon et al.,[20] the exchange between different partially folded conformations of GB1HS#124^{F26A} occur at a time scale of microseconds−milliseconds. Therefore, the above observation supports this notion of slow exchange. These high T_1 values, therefore, are indirectly suggestive of the role played by slow chemical exchange between the conformational species and successive aggregation. Advanced methods can be further employed to get a deep insight into the motional dynamics of the events during aggregation.

3. CONCLUSIONS

This study is a primer for probing into the mechanism of fibrillation using fast and economic methods on unlabeled polypeptide GB1HS #124^{F26A} by real-time experimentation. These results provide a glimpse into the role of side chains in an aggregation mechanism through domain swapping. These studies clearly show the interplay of different intermediates of the subunits during fibrillation. Intermediates during fibrillation were tracked using size-exclusion profile, confirming that the dimer destabilizes into partially folded monomeric form before oligomerization into amyloid fibrillation. Furthermore, the evidence was provided by diffusion NMR which could clearly establish a trend where the stable domain-swapped dimer form of the polypeptide destabilizes and further aggregates to form an amyloid fibril. Relaxation measurements further explain the trend of mobility of side-chain protons which could provide a partial explanation of separation of the dimers, monomers, and intermediate species during size exclusion. Furthermore, investigations could be made to probe dynamics at higher time scales using HD exchange experiments. This could help in the atomistic level investigation of amyloid fibril aggregation. Monitoring the time course of fibrillation in real time using these tools could provide a better perspective to compare the initial fibrillation conditions and the final product of amyloid fibrillation.

4. MATERIALS AND METHODS

4.1. Expression and Purification of GB1HS#124^{F26A}. The mutant GB1HS124^{F26A} containing four mutation sites (L5V/F30V/Y33F/A34F) cloned in plasmid vector pET11a was a kind gift by John M. Louis (NIDDK, NIH, Bethesda, USA). The method for expression and purification of this polypeptide is similar to the protocols developed by Louis et al. and Frank et al.[21,44] The plasmid was transformed into *Escherichia coli* (*E. coli*) BL21 DE3 cells and the polypeptide was expressed in 250 mL of Luria Bertini and M9 minimal culture media using 0.5 mM IPTG. The culture media containing induced *E. coli* cells was incubated at temperature 22 °C with shaking at 600 rpm overnight. Purification of polypeptides was achieved using the standard procedure for GB1 polypeptide purification. The expressed cells were pelleted and resuspended in 10 mL of PBS (1.7 mM KH_2PO_4, 5 mM Na_2HPO_4, 150 mM NaCl, pH = 7.4). The cells were subjected to heat treatment in a water bath at 80 °C for 5 min and was put in an ice-bath for 10 min soon after. The supernatant was collected after centrifugation of the lysed cells at 16 000 rpm for 10 min. Buffer for the polypeptide was exchanged by dialysis against Milli-Q water and subsequently to phosphate buffer (pH-5.5). Dialyzed fraction of the polypeptide was concentrated using Merck-Millipore Centricon Plus-70 (MWCO 3 kDa). The concentrated fraction of the polypeptide was further eluted through an Enrich SEC-70 column in BioLogic Duoflow Quadtech 10 (BioRad laboratories) at a flow rate of 0.3 mL/min. The gel filtration column Enrich SEC-70 was equilibrated in 50 mM sodium phosphate buffer (pH = 5.5) with 0.02% NaN_3. The peak fractions were collected, dialyzed in water, and lyophilized. Polypeptide concentration was determined using a UV−vis spectrophotometer using an extinction coefficient for GB1HS#124^{F26A} (8250 M^{-1} cm^{-1}) and monomeric molecular mass.[44]

4.2. SEC. Elution profiling of polypeptides by SEC was monitored using an Quadtech detector in a Biologic Duoflow FPLC system (BioRad laboratories) at λ = 280 nm. Lyophilized polypeptides were dissolved in 5 mL of Milli-Q water to a concentration of 0.6 mM. 0.5 mL of this solution was syringe filtered and loaded on the Enrich SEC-70 column (BioRad laboratories) equilibrated in 50 mM sodium phosphate buffer (pH = 5.5). The remaining polypeptides in a polypropylene tube were shaken at 600 rpm incubated at 58 °C. 0.5 mL of aliquots were taken out at 12, 36, and 84 h of fibrillation and subjected to size-exclusion profiling after centrifugation at 18 000 rpm in a microcentrifuge tube and filtering the solution through a 0.45 μm PES membrane syringe filter. The SEC-70 column was calibrated using lysozyme (14.5 kDa) and wt protein GB1(6.2 kDa) in phosphate buffer at pH = 5.5.

4.3. DLS Analysis. DLS measurements were performed at 25 °C using a Zetasizer Nano-ZX (Malvern). Scattering peaks less than 0.1 nm radius were ignored. The protein samples at different time points during the course of fibrillation (i.e., 0, 12, 36, and 84 h) were centrifuged at 10 000*g*, and the supernatant was further diluted in sodium phosphate buffer (pH-5.5) to a final concentration 10 μM and measured immediately. Scattering peaks corresponding to radius less than 0.1 nm were ignored.

4.4. Solution NMR Spectroscopy. *4.4.1. Sample Preparation.* Unlabeled lyophilized polypeptide GB1HS#124^{F26A} was reconstituted in 0.6 mL of sodium phosphate buffer prepared in D_2O (pH = 5.5) (Sigma−Merck) to a concentration of 0.6 mM. It was then transferred to a 5 mm diameter Wilmad NMR tubes (Sigma−Merck). The top of the NMR tube was sealed, and the sample in the NMR tube was incubated at 58 °C with shaking at 600 rpm.

4.4.2. Assignment of Side-Chain-Attached ^{1}H NMR Chemical Shifts. All NMR experiments were recorded using Bruker Biospin Avance III at 800 MHz ^{1}H frequency equipped with a 5 mm inverse broadband probe head containing triple channel TCI probe with Z-shielded gradient at 298 K and a

https://doi.org/10.1021/acsomega.1c04223
ACS Omega 2021, 6, 34359−34366

cryoprobe head. For identifying chemical shifts of side-chain-attached protons of amino acid residues of GB1 HS#124^{F26A} 1D ^{1}H NMR with presaturation pulse for water suppression (standard Bruker pulse sequence *zgpr*) at 25 °C and 58 °C, and 2D ^{1}H−^{13}C HSQC (standard Bruker pulse sequence *hsqcetgp*) were recorded for the polypeptide sample in natural abundance at 58 °C. 128 transients for 1D ^{1}H NMR and 40 transients for 2D ^{1}H−^{13}C HSQC were obtained, respectively. The NMR data was processed using Bruker Topspin 4.0.7. The chemical shifts of ^{1}H and ^{13}C for the obtained spectra were compared to that of the existing ^{1}H and ^{13}C NMR assignments data in the BMRB database with access code 5875. The NMR tube containing GB1HS#124^{F26A} polypeptide was placed in the shaker-incubator at 58 °C and 600 rpm and experiments were repeated at 12, 36, and 84 h, respectively, of incubation for fibrillation, acquiring each NMR spectra at same parameters of the experiment.

4.4.3. Diffusion NMR. Diffusion experiments were recorded for ^{1}H nuclei using 2D sequence for bipolar gradient pulse with stimulated echo and longitudinal encoding−decoding (Bruker pulse sequence *ledbpgp2s*).[45] Gradient strength values were taken in range of 2−98% in 16 steps. Gradient length was set to 1.5 ms and diffusion time was set to be 120 ms. 32 transients were obtained for each experiment at time points of 12, 36, and 84 h. All experiments were recorded at 58 °C.

Processing of the diffusion data was performed using Bruker Topspin 4.0.7 and the diffusion coefficients in m^2 s^{-1} were calculated for each of the side-chain proton peaks using dynamic center suite in Bruker Topspin 4.0.7 after curve fitting using the following equation

$$I = I_0 \, e^{-D\gamma^2 g^2 \delta^2 (\Delta - \delta/3)} \quad (1)$$

4.4.4. T_1 Relaxation Measurement. T_1 relaxation time was measured in seconds for all the assigned side-chain-attached protons to assess their motion at the chosen time points during fibrillation. T_1 relaxation time measurement for side-chain-attached protons was carried out using a pseudo 2D inversion recovery experiment for ^{1}H nuclei (Bruker pulse sequence *t1ir*). Relaxation delay was set to 5 s. A series of 22 variable delay values were taken ranging from 10 μs to 10 s. The experiments were acquired at 0, 12, 36, and 84 h, respectively, at 58 °C..

Processing, slicing, and integration of the peaks for side-chain protons were achieved through T_1/T_2 measurement suite in Bruker Topspin 4.0.7. T_1 values were obtained through curve fitting through the equation

$$I_t = I_0 + P \, e^{(-t/T1)} \quad (2)$$

■ ASSOCIATED CONTENT

Supporting Information

The Supporting Information is available free of charge at https://pubs.acs.org/doi/10.1021/acsomega.1c04223.

Tris-tricine SDS-PAGE to track low-molecular weight species during the process of aggregation, NMR spectral assignment of GB1HS#124^{F26A} polypeptide side chain at 58 °C, 2D ^{1}H−^{13}C HSQC NMR spectra of GB1 HS#124^{F26A} at different time points during amyloid fibrillation, Diffusion Coefficient for protons attached to side chain carbons of amino acid residues in GB1HS#124F26A peptide, and T1 Relaxation measurements of side-chain-attached protons during fibrillation (PDF)

■ AUTHOR INFORMATION

Corresponding Authors

Arvind M. Kayastha − *School of Biotechnology, Institute of Science, Banaras Hindu University, Varanasi 221005, Uttar Pradesh;* orcid.org/0000-0002-5090-7159; Email: kayasthabhu@gmail.com

Neeraj Sinha − *Centre of Biomedical Research, SGPGIMS Campus, Lucknow 226014, Uttar Pradesh;* orcid.org/0000-0003-3235-6127; Email: neeraj.sinha@cbmr.res.in

Authors

Renuka Ranjan − *Centre of Biomedical Research, SGPGIMS Campus, Lucknow 226014, Uttar Pradesh; School of Biotechnology, Institute of Science, Banaras Hindu University, Varanasi 221005, Uttar Pradesh*

Nidhi Tiwari − *Centre of Biomedical Research, SGPGIMS Campus, Lucknow 226014, Uttar Pradesh; Department of Chemistry, Institute of Science, Banaras Hindu University, Varanasi 221005, Uttar Pradesh*

Complete contact information is available at: https://pubs.acs.org/10.1021/acsomega.1c04223

Notes

The authors declare no competing financial interest.

■ ACKNOWLEDGMENTS

R.R. and N.T. acknowledges the Senior Research Fellowship from the Council of Scientific and Industrial Research, New Delhi, India, for funding (file no. 09/916(0085)/2015-EMR-I, 09/916(0086)/2016-EMR-I). N.S. acknowledges financial assistance from SERB India (Grant no. EMR/2015/001758). We thank Ritu Raj and Dr. Dinesh Kumar Gupta, Centre of Biomedical Research for assistance in conducting experiments. We acknowledge Dr. Smriti Priya, CSIR-Indian Institute of Toxicology for performing DLS measurements.

■ REFERENCES

(1) Sipe, J. D.; Cohen, A. S. Review: History of the Amyloid Fibril. *J. Struct. Biol.* **2000**, *130*, 88−98.

(2) Žerovnik, E.; Stoka, V.; Mirtič, A.; Gunčar, G.; Grdadolnik, J.; Staniforth, R. A.; Turk, D.; Turk, V. Mechanisms of Amyloid Fibril Formation - Focus on Domain-Swapping. *FEBS J.* **2011**, *278*, 2263−2282.

(3) Cawood, E. E.; Karamanos, T. K.; Wilson, A. J.; Radford, S. E. Visualizing and Trapping Transient Oligomers in Amyloid Assembly Pathways. *Biophys. Chem.* **2021**, *268*, 106505.

(4) Bennett, M. J.; Sawaya, M. R.; Eisenberg, D. Deposition Diseases and 3D Domain Swapping. *Structure* **2006**, *14*, 811−824.

(5) Galzitskaya, O. V. Regions Which Are Responsible for Swapping Are Also Responsible for Folding and Misfolding. *Open Biochem. J.* **2011**, *5*, 27−36.

(6) Liu, Y.; Eisenberg, D. 3D Domain Swapping: As Domains Continue to Swap. *Protein Sci.* **2002**, *11*, 1285−1299.

(7) Gill, B. Trading Places. *Embroidery* **2010**, *61*, 30−33.

(8) Gronenborn, A. M. Protein Acrobatics in Pairs - Dimerization via Domain Swapping. *Curr. Opin. Struct. Biol.* **2009**, *19*, 39−49.

(9) Jaskólski, M. 3D Domain Swapping, Protein Oligomerization, and Amyloid Formation. *Acta Biochim. Pol.* **2001**, *48*, 807−827.

(10) Medina, E.; Córdova, C.; Villalobos, P.; Reyes, J.; Komives, E. A.; Ramírez-Sarmiento, C. A.; Babul, J. Three-Dimensional Domain

Swapping Changes the Folding Mechanism of the Forkhead Domain of FoxP1. *Biophys. J.* **2016**, *110*, 2349−2360.
(11) Wahlbom, M.; Wang, X.; Lindström, V.; Carlemalm, E.; Jaskolski, M.; Grubb, A. Fibrillogenic Oligomers of Human Cystatin C Are Formed by Propagated Domain Swapping. *J. Biol. Chem.* **2007**, *282*, 18318−18326.
(12) Yang, S.; Levine, H.; Onuchic, J. N. Protein Oligomerization through Domain Swapping: Role of Inter-Molecular Interactions and Protein Concentration. *J. Mol. Biol.* **2005**, *352*, 202−211.
(13) Shewmaker, F.; McGlinchey, R. P.; Wickner, R. B. Structural Insights into Functional and Pathological Amyloid. *J. Biol. Chem.* **2011**, *286*, 16533−16540.
(14) Schlunegger, M.; Bennett, M.; Eisenberg, D. Oligomer Formation by 3D Domain Swapping: A Model for Protein Assembly and Misassembly. *Adv. Protein Chem.* **1997**, *50*, 61−122.
(15) Rousseau, F.; Schymkowitz, J.; Itzhaki, L. S. Implications of 3D Domain Swapping for Protein Folding, Misfolding and Function. *Adv. Exp. Med. Biol.* **2012**, *747*, 137−152.
(16) Jee, J.; Ishima, R.; Gronenborn, A. M. Characterization of Specific Protein Association By15N CPMG Relaxation Dispersion NMR: The GB1A34F Monomer-Dimer Equilibrium. *J. Phys. Chem. B* **2008**, *112*, 6008−6012.
(17) Sirota, F. L.; Héry-Huynh, S.; Maurer-Stroh, S.; Wodak, S. J. Role of the Amino Acid Sequence in Domain Swapping of the B1 Domain of Protein G. *Proteins: Struct., Funct., Genet.* **2008**, *72*, 88−104.
(18) Ramirez-Alvarado, M.; Merkel, J. S.; Regan, L. A Systematic Exploration of the Influence of the Protein Stability on Amyloid Fibril Formation in Vitro. *Proc. Natl. Acad. Sci. U.S.A.* **2000**, *97*, 8979−8984.
(19) Byeon, I.-J. L.; Louis, J. M.; Gronenborn, A. M. A Protein Contortionist: Core Mutations of GB1 That Induce Dimerization and Domain Swapping. *J. Mol. Biol.* **2003**, *333*, 141−152.
(20) Byeon, I.-J. L.; Louis, J. M.; Gronenborn, A. M. A Captured Folding Intermediate Involved in Dimerization and Domain-Swapping of GB1. *J. Mol. Biol.* **2004**, *340*, 615−625.
(21) Louis, J. M.; Byeon, I.-J. L.; Baxa, U.; Gronenborn, A. M. The GB1 Amyloid Fibril: Recruitment of the Peripheral β-Strands of the Domain Swapped Dimer into the Polymeric Interface. *J. Mol. Biol.* **2005**, *348*, 687−698.
(22) Li, J.; Hoop, C. L.; Kodali, R.; Sivanandam, V. N.; van der Wel, P. C. A. Amyloid-like Fibrils from a Domain-Swapping Protein Feature a Parallel, in-Register Conformation without Native-like Interactions. *J. Biol. Chem.* **2011**, *286*, 28988−28995.
(23) Brender, J. R.; Ghosh, A.; Kotler, S. A.; Krishnamoorthy, J.; Bera, S.; Morris, V.; Sil, T. B.; Garai, K.; Reif, B.; Bhunia, A.; Ramamoorthy, A. Probing Transient Non-Native States in Amyloid Beta Fiber Elongation by NMR. *Chem. Commun.* **2019**, *55*, 4483−4486.
(24) Li, P.-C.; Huang, L.; Makarov, D. E. Mechanical Unfolding of Segment-Swapped Protein G Dimer: Results from Replica Exchange Molecular Dynamics Simulations. *J. Phys. Chem. B* **2006**, *110*, 14469−14474.
(25) Ding, K.; Louis, J. M.; Gronenborn, A. M. Insights into Conformation and Dynamics of Protein GB1 during Folding and Unfolding by NMR. *J. Mol. Biol.* **2004**, *335*, 1299−1307.
(26) Tubert, P.; Laurents, D. V.; Ribó, M.; Bruix, M.; Vilanova, M.; Benito, A. Interactions Crucial for Three-Dimensional Domain Swapping in the HP-RNase Variant PM8. *Biophys. J.* **2011**, *101*, 459−467.
(27) Nguyen, P. H.; Ramamoorthy, A.; Sahoo, B. R.; Zheng, J.; Faller, P.; Straub, J. E.; Dominguez, L.; Shea, J.-E.; Dokholyan, N. v.; de Simone, A.; Ma, B.; Nussinov, R.; Najafi, S.; Ngo, S. T.; Loquet, A.; Chiricotto, M.; Ganguly, P.; McCarty, J.; Li, M. S.; Hall, C.; Wang, Y.; Miller, Y.; Melchionna, S.; Habenstein, B.; Timr, S.; Chen, J.; Hnath, B.; Strodel, B.; Kayed, R.; Lesné, S.; Wei, G.; Sterpone, F.; Doig, A. J.; Derreumaux, P. Amyloid Oligomers: A Joint Experimental/Computational Perspective on Alzheimer's Disease, Parkinson's Disease, Type II Diabetes, and Amyotrophic Lateral Sclerosis. *Chem. Rev.* **2021**, *121*, 2545−2647.
(28) Nandwani, N.; Surana, P.; Negi, H.; Mascarenhas, N. M.; Udgaonkar, J. B.; Das, R.; Gosavi, S. A Five-Residue Motif for the Design of Domain Swapping in Proteins. *Nat. Commun.* **2019**, *10*, 452.
(29) Grigolato, F.; Arosio, P. The Role of Surfaces on Amyloid Formation. *Biophys. Chem.* **2021**, *270*, 106533.
(30) Ivanova, M. I.; Lin, Y.; Lee, Y.-H.; Zheng, J.; Ramamoorthy, A. Biophysical Processes Underlying Cross-Seeding in Amyloid Aggregation and Implications in Amyloid Pathology. *Biophys. Chem.* **2021**, *269*, 106507.
(31) Kotler, S. A.; Brender, J. R.; Vivekanandan, S.; Suzuki, Y.; Yamamoto, K.; Monette, M.; Krishnamoorthy, J.; Walsh, P.; Cauble, M.; Holl, M. M. B.; Marsh, E. N. G.; Ramamoorthy, A. High-Resolution NMR Characterization of Low Abundance Oligomers of Amyloid-β without Purification. *Sci. Rep.* **2015**, *5*, 11811.
(32) Sahoo, B. R.; Cox, S. J.; Ramamoorthy, A. High-Resolution Probing of Early Events in Amyloid-β Aggregation Related to Alzheimer's Disease. *Chem. Commun.* **2020**, *56*, 4627−4639.
(33) Moschen, T.; Tollinger, M. A Kinetic Study of Domain Swapping of Protein L. *Phys. Chem. Chem. Phys.* **2014**, *16*, 6383−6390.
(34) Ratha, B. N.; Ghosh, A.; Brender, J. R.; Gayen, N.; Ilyas, H.; Neeraja, C.; Das, K. P.; Mandal, A. K.; Bhunia, A. Inhibition of Insulin Amyloid Fibrillation by a Novel Amphipathic Heptapeptide: Mechanistic Details Studied by Spectroscopy in Combination with Microscopy. *J. Biol. Chem.* **2016**, *291*, 23545−23556.
(35) Chen, H.-Y.; Ragavan, M.; Hilty, C. Protein Folding Studied by Dissolution Dynamic Nuclear Polarization. *Angew. Chem., Int. Ed.* **2013**, *125*, 9362−9365.
(36) Ragavan, M.; Iconaru, L. I.; Park, C.-G.; Kriwacki, R. W.; Hilty, C. Real-Time Analysis of Folding upon Binding of a Disordered Protein by Using Dissolution DNPNMRSpectroscopy. *Angew. Chem., Int. Ed.* **2017**, *56*, 7070−7073.
(37) Krishnamoorthy, J.; Brender, J. R.; Vivekanandan, S.; Jahr, N.; Ramamoorthy, A. Side-Chain Dynamics Reveals Transient Association of Aβ1-40 Monomers with Amyloid Fibers. *J. Phys. Chem. B* **2012**, *116*, 13618−13623.
(38) Wang, J.; Yamamoto, T.; Bai, J.; Cox, S. J.; Korshavn, K. J.; Monette, M.; Ramamoorthy, A. Real-Time Monitoring of the Aggregation of Alzheimer's Amyloid-β: Via 1H Magic Angle Spinning NMR Spectroscopy. *Chem. Commun.* **2018**, *54*, 2000−2003.
(39) Karamanos, T. K.; Kalverda, A. P.; Thompson, G. S.; Radford, S. E. Mechanisms of Amyloid Formation Revealed by Solution NMR. *Prog. Nucl. Magn. Reson. Spectrosc.* **2015**, *88−89*, 86−104.
(40) Price, W. S.; Tsuchiya, F.; Arata, Y. Lysozyme Aggregation and Solution Properties Studied Using PGSE NMR Diffusion Measurements. *J. Am. Chem. Soc.* **1999**, *121*, 11503−11512.
(41) Lin, M. F.; Larive, C. K. Detection of Insulin Aggregates with Pulsed-Field Gradient Nuclear Magnetic Resonance Spectroscopy. *Anal. Biochem.* **1995**, *229*, 214−220.
(42) Buevich, A. v.; Baum, J. Residue-Specific Real-Time NMR Diffusion Experiments Define the Association States of Proteins during Folding. *J. Am. Chem. Soc.* **2002**, *124*, 7156−7162.
(43) Rabdano, S. O.; Bystrov, S. S.; Luzik, D. A.; Chizhik, V. I. NMR Relaxation of Nuclei of Buffer as a Probe for Monitoring Protein Solutions Including Aggregation Processes. *Appl. Magn. Reson.* **2020**, *51*, 1653−1668.
(44) Frank, M. K.; Dyda, F.; Dobrodumov, A.; Gronenborn, A. M. Core Mutations Switch Monomeric Protein GB1 into an Intertwined Tetramer. *Nat. Struct. Mol. Biol.* **2002**, *9*, 877−885.
(45) Wu, D. H.; Chen, A. D.; Johnson, C. S. An Improved Diffusion-Ordered Spectroscopy Experiment Incorporating Bipolar-Gradient Pulses. *J. Magn. Reson., Ser. A* **1995**, *115*, 260−264.
(46) Soong, R.; Brender, J. R.; Macdonald, P. M.; Ramamoorthy, A. Association of Highly Compact Type II Diabetes Related Islet Amyloid Polypeptide Intermediate Species at Physiological Temperature Revealed by Diffusion NMR Spectroscopy. *J. Am. Chem. Soc.* **2009**, *131*, 7079−7085.

https://doi.org/10.1021/acsomega.1c04223
ACS Omega 2021, 6, 34359−34366